9. Williams D. B., Carter C. B. Transmission Electron Microscopy. V. 3. – N. Y.: Plenum Press, 1996. – 201 p.
10. Определение структурной неоднородности кристаллов искусственных алмазов методом Кикучи-дифракции / М. Д. Борча, С. В. Баловсяк, Я. Д. Гарабажив и др. // Металлофизика и новейшие технологии. – 2009. –**31**. – № 7. – С. 911–925.
11. Глазов В. М., Вигдорович В. Н. Микротвердость металлов и полупроводников. – М.: Металлургия, 1969. – 248 с.
12. Клюев Ю.А., Непша В.И., Безруков Г.Н. Инфракрасные спектры синтетических алмазов // Алмазы. – 1972. – Вып. 5. – С. 5–10.
13. Начальная Т.А., Подзярей Г.А., Прихна А.И. и др. Спектроскопические исследования поликристаллов, спеченных из алмазных микропорошков // Сверхтвердые материалы. – 1981. – № 3. – С. 23–27.
14. О состоянии примесного азота в искусственном алмазе / Е. В. Соболев, Ю. А. Литвин, Н. Д. Самсоненко и др. // ФТТ. – 1968. – **10**. – №7. – С. 2266–2268.
15. Chrenko R. M., Strong H. M., Tuft R. E. Dispersed paramagnetic nitrogen content in large laboratory diamond // Phil. Mag. – 1971. – **23**. – N 182. – P. 313–318.
16. Выращивание эпитаксиальных алмазных плёнок и кристаллов в микроволновой плазме / А. П. Большаков, В. Г. Ральченко, А. В. Польский и др. // Рос. хим. журн. – 2012. – № 1–2 (в печати).
17. Iakoubovskii K., Adriaenssens G J and Nesladek M. Photochromism of vacancy-related centres in diamond // J. Phys.: Condens. Matter. – 2000. – N 12. – P. 189–199.
18. Characterization of nitrogen doped chemical vapor deposited single crystal diamond before and after high pressure, high temperature annealing / S. J. Charles, J. E. Butler, B. N. Feygelson et al. // Phys. Stat. Sol. (a) – 2004. – **201**. – N 11. – P. 2473–2485.
19. Microwave plasma-assisted photoluminescence enhancement in nitrogen-doped ultrananocrystalline diamond film / Yu Lin Liu, Kien Wen Sun, Yi Jie Lin et. al.//Aip Advances. – 2012. – 2, 022145. – Doi: 10.1063/1.4727743.

*Поступила 15.06.12*

УДК 621.9:621.762-539.27

**M. Szutkowska**, Prof. Ph. D., D. Sc.; **M. Rozmus**, Ph. D.**; P. Figiel**, Ph. D.;
**L. Jaworska**, Prof. Ph. D., D. Sc.

*Institute of Advanced Manufacturing Technology, Krakow, Poland*

## MECHANICAL PROPERTIES OF DIAMOND–$TiB_2$ COMPOSITES

*The presented paper characterizes the basic mechanical and physical properties of sintered diamond-titanium diboride (submicro) and diamond-titanium diboride (nano) composites. The effect of reduction of powder size from the submicron scale to the nano scale of the ceramic bonding phase ($TiB_2$) in diamond composites on selected mechanical properties (Young's modulus, Vickers hardness, fracture toughness, coefficient of friction) has been reported. Composites were prepared from initial powders of diamond (MDA36, Element Six) with addition of 10 mass % submicron $TiB_2$ (H.C. Starck F) and 10 mass % nanopowder $TiB_2$ (American Elements). Compacts were sintered at pressure 8±0,5 GPa and 2233±50 K using the high pressure-high temperature Bridgman type apparatus. These investigations allow the possibility of using this materials to be enhacced as ceramic tool materials, in particular as burnishing tools.*

***Key words**: diamond composite, $TiB_2$ bonding phase, HP-HT sintering, fracture toughness, Vickers hardness.*

**Introduction**

Diamond composites have a wide range of compositions and applications. They have been often referred to as PCD (polycrystalline diamond), PDC (polycrystalline diamond compact/cutter) and TSP (thermally stable polycrystalline diamond composite, sometimes represented as TSDC) [1]. Polycrystalline superhard cutting materials are obtained by sintering together graded diamond or cubic boron nitride powders with a metallic binder or catalyst, at temperatures and pressures similar to those used in their original synthesis. The resultant compact is circular, with diameter and thickness depending on the chamber size and load, and can be cut into a large variety of shapes for cutting tools, and special wear-resistant parts [2]. The type of the bonding phase has a significant influence on the microstructure and mechanical properties of diamond compacts. The most popular PCD are those with cobalt, due to good wetting of diamond crystallites by this metal.

PCD with cobalt is a subject thermally stable only up to 1173 K because cobalt is a metal catalyst for the graphite – diamond and diamond – graphite conversion process [3, 4]. Due to high toxicity of cobalt, the exposure to metal powders or to metal dust during the cutting processes is particularly hazardous. Also in the sintered diamond with a metal binding phase, which forms internal lattice carbides, usually non-stoichiometric compounds are formed. As a result of the non-stochiometric chemical composition there is a significant damage of structure which affects the deterioration of mechanical properties of the material, especially reducing its hardness. Studies of the sintering of diamond powders with the non-metalic binding phase were carried out earlier by L. Jaworska [5].

Attractive properties of $TiB_2$ made it the subject of research for manufacturing tool components for several years. Titanium diboride with high melting point (3498 K), low density (4.5 $g/cm^3$), high hardness (25 GPa), good thermal conductivity (96 W/m·K), high electrical conductivity ($22 \cdot 10^6$ Ω·cm) and considerable chemical stability is one of the candidates for high temperature structural and wear applications. This unique combination of properties of $TiB_2$-based materials makes them suitable for a wide range of technological applications, such as armour materials, wear components, conductive coatings, cathode materials for the Hall-Herroult cell, aluminium evaporation boats and electro discharge machining (EDM) electrodes [6–9]. Boride materials of $MeB_2$ type have a high value of critical stress intensity factor $K_{IC}$, approximately from 5 to 7 $MPa \cdot m^{1/2}$ [5]. Titanium diboride, due to its high hardness and poor sinterability was sintered with metallic additions. The presence of metals increases toughness and sinterability of the $TiB_2$ ceramics, but the metal addition affects binder corrosion at elevated temperatures [10]. The existence of the covalent bonding is the reason of low ductility, high hardness and high melting point of $TiB_2$. Due to its high electrical conductivity $TiB_2$ can be easily machined using the technique of electrical discharge machining. This advantage is used during shaping the cutting edge of tools made of the diamond-$TiB_2$ composite. The use of hard phase binder such as $TiB_2$ in the sintering process for diamond powders is a kind of innowation because for commercial diamond materials ductile binding phases are used for example Co or Ni. These materials provide pseudoisostatic pressure distribution during the HP-HT process of diamond. During the HP-HT sintering in the pressure range corresponding to the thermodynamic stability of diamond, the allotropic transformation process occurs from diamond to graphite on the surface bordering with pores. A removal of voids is crucial, as otherwise the diamond particle is only locally bound with the binder or finer diamond, keeping the diamond in a compressive force state, i.e. preserving diamond stability. The application of nanometer binding phase particles that can fill the voids between grains of diamond may be very important in the sintering process.

The aim of this study is to obtain the diamond-$TiB_2$ ceramic composite with submicrometer and nanometer powders of $TiB_2$, using the High Pressure-High Temperature (HP-HT) process. Mechanical and physical properties of composites with nano $TiB_2$ will be compared to the composites with submicrometer powders.

**Experimental procedure**

The following commercially available powders were used to prepare the mixtures:

- synthetic diamond powders (Element Six): MDA 36; 3–6 μm grain size;

- titanium diboride submicrometer powder (H.C. Starck F): 2.5–3.5 μm grain size;
- titanium diboride nanopowder (American Elements): about 100 nm grain size.

The above powders of $TiB_2$ in the amount of 10 mass % with diamond powder were mixed in acetone using Turbula mixer and then the powders were dried. After drying the mixtures, were preliminarily consolidated into pellets of 15 mm diameter and 5 mm height under the pressure of about 200 MPa. The green compacts were placed into the internal graphite heater in a special ceramic gasket assembly for sintering. The samples were sintered using the HP-HT method at the pressure of 8±0.5 GPa and temperature of 2233±50 K using the Bridgman type toroidal apparatus (fig. 1). The sintering process lasted 25 seconds. After sintering, the materials were subjected to a study of physical and mechanical properties.

*Fig. 1. View of the HP–HT Bridgman type apparatus*

Metallographic specimens were prepared using the Struers apparatus with polishing agents. Apparent density ρ and porosity were measured using the hydrostatic method. Young's modulus $E$ measurements of the sintered samples were also taken, using the ultrasonic method measurements of the transition speed of transverse and longitudinal waves, by the Panametrics Epoch III flaw detector. Elasticity modulus (Young's modulus) values are the characteristic parameters for many technical materials. In the case of ceramics the elasticity modulus can be considered as the main parameter, which determines their properties as well as suitability for the given applications. The calculations are carried out according to formula

$$E = \rho V_T^2 \frac{3V_L^2 - 4V_T^2}{V_L^2 - V_T^2}, \quad (1)$$

where $V_L$ – velocity of the longitudinal wave; $V_T$ – velocity of the transversal wave.

Hardness was determined by the Vickers method at a load of 9.8 N using a digital hardness tester (future Tech. Corp. FM-7).

Fracture toughness $K_{IC}$ was measured by the conventional method based on the single-edge notched bending (SENB) specimens. Relationship of $K_{IC} = f(c)$ is given by equations

$$K_{1C} = 1.5\frac{P_c S}{W^2 B} Yc^{1/2} \tag{2}$$

$$Y = \frac{\sqrt{\Pi}}{(1-\beta)^{\frac{3}{2}}}\left[0{,}3738\beta + (1-\beta)\sum_{i,j=0}^{4} A_{ij}\beta^i\left(\frac{W}{S}\right)^j\right] \tag{3}$$

where $P_c$ – critical load; $S$ – support span; $W$ – width; $B$ – specimen thickness; $Y$ – geometric function; $c$ – crack length; $\beta - c/W$, $A_{ij}$ coefficients [11].

Coefficients of friction for the diamond–$TiB_{2sub}$ and diamond–$TiB_{2nano}$ composites in sliding contact $Si_3N_4$ ceramic were measured in ball-on-disc tests, using CETR UMT-MT universal mechanical tester. In the ball-on-disc method, sliding contact is conducted by pushing a ball specimen onto a rotating disc specimen under a constant load. For measurements of values of friction coefficient the non-ferrous pair of friction materials was used which corresponds to the assumption that diamond tool material cannot be used for machining of alloys containing iron (and other materials from the iron group), due to the solubility of carbon in iron.

Friction coefficient was calculated from equation

$$\mu = \frac{F_t}{F_n} \tag{4}$$

where $F_t$ – measured friction force; $F_n$ – applied normal force.

For the materials after grinding and ionic precision etching the surface (equipment model 682 PECS Gatan) of the sintering compacts was analyzed using the JEOL JSM-6460LV scanning electron microscope.

**Experimental results and their discussion**

The results of measurements of ρ, $E$, Poisson's number $v$, Vickers hardness $HV1$, $K_{IC}$ and $\mu$ of the diamond-$TiB_2$ and diamond-$TiB_{2nano}$ samples obtained by HP-HT sintering are given in Table.

**Selected results of the mechanical and physical properties of the diamond-$TiB_2$ and diamond-$TiB_{2nano}$ composites obtained by HP-HT sintering**

| Sample | Density, g/cm$^3$ | Young's modulus, GPa | Poisson's number | Vickers hardness, GPa | Fracture toughness, MPa·m$^{1/2}$ | Coefficient of friction |
|---|---|---|---|---|---|---|
| 10 mass % submicrometer titanium diboride | | | | | | |
| $DTiB_{2sub}$ | 3,35 | 569 | 0,10 | 49,7 | 6,72 | 0,26 ± 0,04 |
| 10 mass % nanometer titanium diboride | | | | | | |
| $DTiB_{2nano}$ | 3,32 | 561 | 0,08 | 46,3 | 10,4 | 0,11 ± 0,04 |

In the case of diamond composites with submicrometer $TiB_2$ as a binding phase, apparent density obtained after sintering is about 3.40 g/cm$^3$, while the highest value of apparent density for the sample with nanometer $TiB_2$ as a binding phase is 3.40 g/cm$^3$. The highest value of Young's modulus is equal to 569 GPa for the diamond–$TiB_2$ samples and 561 GPa for the diamond–$TiB_{2nano}$ samples. The average value of Vickers hardness for diamond composites with submicrometer $TiB_2$ is equal to 49.7 GPa. A lower (about 7 %) value of the Vickers hardness for the diamond–$TiB_{2nano}$ samples was obtained. In the case of fracture toughness, the higher value was obtained for the diamond–$TiB_{2nano}$ samples (10.4 MPa·m$^{1/2}$) in comparison to the diamond–$TiB_2$ (6.72 MPa·m$^{1/2}$).

The curves (fig. 2) presented the results of measurements of friction coefficients for the diamond–$TiB_2$ and diamond–$TiB_{2nano}$ samples for the $Si_3N_4$ ceramic ball contact. The values of friction coefficient μ of the tested composites at the contact with the $Si_3N_4$ ceramic ball exhibit lower vales (μ = 0.11–0.15) for the diamond–$TiB_{2nano}$ samples in comparison to the diamond–$TiB_2$ samples.

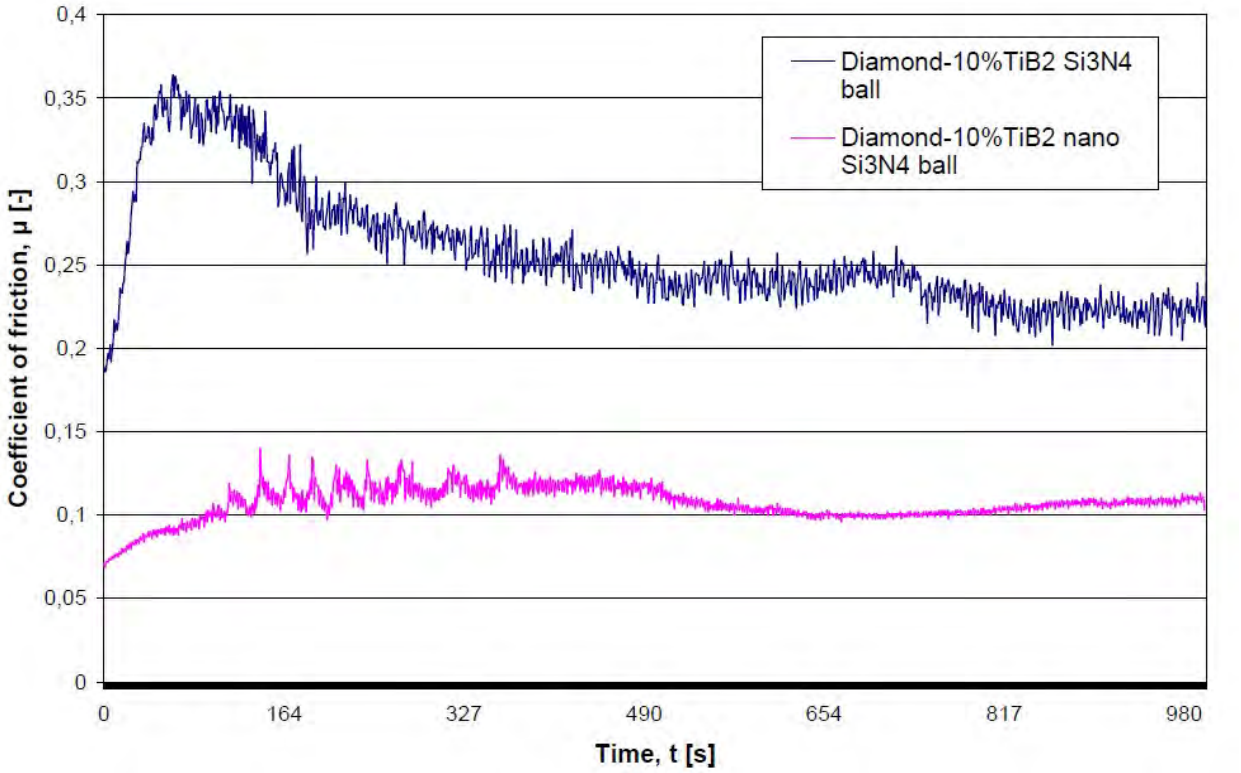


*Fig. 2. Coefficient of friction of selected diamond–TiB2 and diamond–TiB2nano composites*

Fig. 3 shows the representative microstructures of the diamond–$TiB_2$ and diamond–$TiB_{2nano}$ composites sintered by the HP-HT process. In both microstructures the diamond–$TiB_2$ (fig. 3, *a*) and the diamond-$TiB_2$ (fig. 3, *b*) agglomerates are visible. A part from the presence of agglomerates the materials are homogeneous.

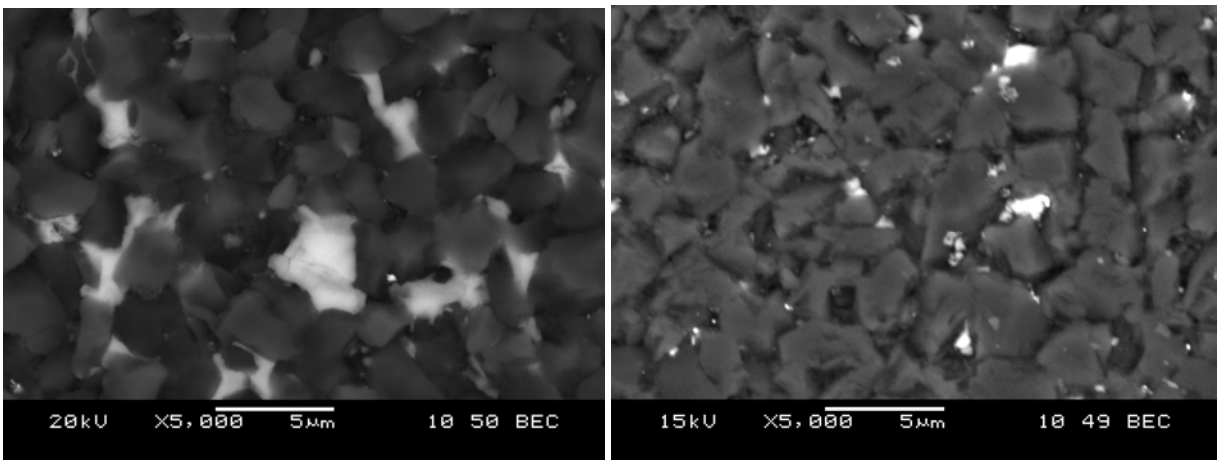


*a* *b*

*Fig. 3. SEM micrographs of diamond–TiB2 (a) and diamond–TiB2nano (b) samples (the titanium diboride crystallites are characterized by white colour)*

**Conclusions**

The paper presented the method of sintering diamond with the submicrometer $TiB_2$ and nanometer $TiB_2$ powder as a bonding phase by the High Pressure-High Temperature method. The effect of powder size from the submicron scale to the nano scale of $TiB_2$ on selected mechanical properties was studied. The studies of mechanical and physical properties included relative density, Young's modulus, Poisson's number, Vickers hardness and fracture toughness. Also, friction

coefficients were measured and microscopic observations were carried out. Mechanical and physical properties were similar for the diamond–$TiB_2$ and the diamond–$TiB_{2nano}$ composites whereas the value of Vickers hardness was slightly higher for the diamond–$TiB_2$ composites than for the diamond–$TiB_{2nano}$. For the value of fracture toughness, a higher value was obtained for the diamond–$TiB_{2nano}$ composites. The diamond–$TiB_{2nano}$ composite reveals higher values of friction coefficient at the contact with the $Si_3N_4$ ball than the diamond-$TiB_{2nano}$ composite. Both submicrometer and nanometer $TiB_2$ powders have a tendency to form agglomerates which can be visible in SEM micrograps of microstructures.

**Acknowledgments**

This work was supported by the Ministry of Science and Higher Education, Republic of Poland (Project no. NN508 480138) 2010-2013.

*Наведені основні механічні та фізичні властивості спечених композитів на основі алмазу з додаванням субмікро- та нано-дибориду титану. Вивчено вплив розміру частинок порошку від субмікронного до нано-рівня в керамічній ($TiB_2$) складовій алмазних композитів на їх механічні властивості (модуль Юнга, твердість за Віккерсом, в'язкість руйнування, коефіцієнт тертя). Композити були отримані з вихідних порошків алмазу (MDA36, Element Six) з додаванням 10 мас. % субмікронного $TiB_2$ (HC Starck F) або 10 мас. % нанопорошку $TiB_2$ (American Elements). Зразки спечені при тиску 8±0,5 ГПа і температурі 2233±50 К в апараті високого тиску типу тороїд. Результати досліджень вказують на можливість використання одержаних композитів як інструментальних матеріалів підвищеної якості, зокрема в інструментах для вигладжування.*

***Ключові слова:*** *композит алмаз–$TiB_2$, зв'язуюча фаза, спікання при високих тисках і температурах, в'язкість руйнування, твердість за Віккерсом.*

*Приведены основные механические и физические свойства спеченных композитов на основе алмаза с добавками субмикро- и нано-диборида титана. Изучено влияние размера частиц порошка от субмикронного до нано-уровня в керамической ($TiB_2$) составляющей алмазных композитов на их механические свойства (модуль Юнга, твердость по Виккерсу, вязкость разрушения, коэффициент трения). Композиты были получены из исходных порошков алмаза (MDA36, Element Six) с добавлением 10 масс. % субмикронного $TiB_2$ (HC Starck F) или 10 масс. % нанопорошка $TiB_2$ (American Elements). Образцы были спечены при давлении 8±0,5 ГПа и температуре 2233±50 К в аппарате высокого давления типа тороид. Результаты исследований указывают на возможность использования полученных композитов в качестве улучшенных инструментальных материалов, в частности в выглаживающих инструментах.*

***Ключевые слова:*** *композит алмаз–$TiB_2$, связующая фаза, спекание при высоких давлениях и температурах, вязкость разрушения, твердость по Виккерсу.*

**References**

1. Boland N.J. Microstructural characterization and wear behaviour of diamond composite materials // Mater., – 2010. – N 3. – P. 1390–1419.
2. Brookes K.J.A. Hardmetals and other hard materials // European Powder Metallurgy Association (EPMA). – 1992. – P. 183–186.
3. Diamond compostes with non metal bonding phases for cutting tools applications / L. Jaworska, M. Szutkowska, J. Wszołek et al. // Tooling materials and their applications from research to market: proceedings of 7th International Tooling Conference, Politechnico di Torino. – 2006. – N 1. – P. 685–692.
4. Akashi T., Sawaoka A.B. Shock consolidation of diamond powders // J. of Mater. Sci. – 1987. – N 22. – P. 3276–3286.

5. Jaworska L. Diamond-ceramic bonding phase composites for application in cutting tools // Ceramic Mater. – 2011. – N 63. – P. 131–137.
6. Mukhopadhyaya A., Raju G.B., Basu B., Suri A.K. Correlation between phase evolution, mechanical properties and instrumented indentation response of $TiB_2$-based ceramics // J. of the European Ceramic Society. – 2009. –N 29. – P. 505–516.
7. Gua M., Huangb C., Xiao S., Liu H. Improvements in mechanical properties of $TiB_2$ ceramics tool materials by the dispersion of $Al_2O_3$ particles // Mater. Sci. and Eng., A. – 2008. – N 486. – P. 167–170.
8. Kalfagiannis N., Volonakis G., Tsetseris L., Logothetidis S. Excess of boron in $TiB_2$ superhard thin films: a combined experimental and ab initio study // J. of Phys., D: Applied Phys. – 2011. – N 44. – P. 1–7.
9. Subramanian C., Murthy T., Suri A. Synthesis and consolidation of titanium diboride // Int. J. of Refractory Metals and Hard Mater. – 2007. – N 25. – P. 345–350.
10. De Mestral F., Thevenot F. Ceramic composites: $TiB_2$–TiC–SiC – part I – properties and microstructures in the ternary system // J. of Mater. Sci. – 1991. – N 26. – P. 5547–5560.
11. Szutkowska M., Smuk B., Boniecki M. Titanium carbide reinforced composite tool ceramics based on alumina // Advances in Science and Technology. – 2010. – N 65. – P. 50–55.

*Поступила 05.06.12*

УДК 666.233

**В. Ю. Долматов,** канд. хим. наук

*ФГУП «Специальное конструкторско-технологическое бюро «Технолог», г. Санкт-Петербург, Россия*

## К ВОПРОСУ МЕХАНИЗМА ОБРАЗОВАНИЯ ДЕТОНАЦИОННОГО НАНОАЛМАЗА

*Предложен новый механизм образования частиц наноалмаза при детонационном синтезе. Схема процесса следующая: распад молекул тринитротолуола (ТНТ) на радикалы $CH_3^{\bullet}$, радикалоподобный димер $C_2^{\bullet}$ и молекул гексогена на $C_2^{\bullet}$; одновременное образование циклогексана из $C_2^{\bullet}$ молекулы адамантана в ионизированной форме; взаимодействие алмазоподобного ядра (иона адамантана) с метильной и другими моноуглеродными радикалами; рост частицы ДНА аналогично CVD-процессу. Ионизированная молекула адамантана зарождается в диапазоне от середины зоны химпика до плоскости Чепмена–Жуге, алмазная частица увеличивается в начальной стадии изоэнтропийного (тейлоровского) расширения газообразных продуктов детонации, захватывающих твердые частицы углерода.*

***Ключевые слова:*** *механизм образования, ударная волна, зона химпика, тринитротолуол, детонационный наноалмаз, радикалы, циклогексан, адамантан.*

Теория процесса, приводящего к образованию частиц детонационного наноалмаза (ДНА), до сих пор носит дискуссионный характер. Тем не менее, результаты анализа собственных данных и данных других авторов в основном по результатам подрыва сплава тротила с гексогеном (~50/50), позволяет постепенно подходить к пониманию механизма образования ДНА.

Детонационная волна представляет собой единый комплекс ударной волны, на фронте которой начинается разложение взрывчатого вещества (ВВ), зоны химической реакции (химпика), следующей за ударной волной и заканчивающейся в плоскости Чепмена–Жуге,